From quantum to classical: Schrödinger cats, entanglement, and decoherence

2016 Phys. Scr. 91 063013

(http://iopscience.iop.org/1402-4896/91/6/063013)

IOP Publishing | Royal Swedish Academy of Sciences Physica Scripta

Phys. Scr. **91** (2016) 063013 (9pp) doi:10.1088/0031-8949/91/6/063013

Invited Comment

From quantum to classical: Schrödinger cats, entanglement, and decoherence

L Davidovich

Instituto de Física, Universidade Federal do Rio de Janeiro, PO Box 68528, Rio de Janeiro, RJ 21941-972, Brazil

E-mail: ldavid@if.ufrj.br

Received 7 January 2016
Accepted for publication 5 May 2016
Published 25 May 2016

Abstract

Since the beginning of quantum physics, the relation between the properties of the microscopic quantum and the macroscopic classical world has been an important source for the development of the theory, and has led to new insights on the role of the environment in the transition from quantum to classical physics. Decoherence affects both coherence and entanglement of open systems. Quantum optics and cavity quantum electrodynamics have allowed detailed investigations of this phenomenon, within the framework of microwaves and light waves. In this paper, I present a personal account of theoretical and experimental developments that have led to the probing of the subtle frontier between quantum and classical phenomena.

Keywords: entanglement, decoherence, Schrödinger cat, quantum–classical

(Some figures may appear in colour only in the online journal)

1. Introduction: light, the quantum, and the classical

Light was at the onset of quantum physics, and continues to be a powerful tool to investigate subtle properties of the quantum world and, in particular, the long-standing problem of the quantum–classical transition. Coherence and entanglement are conspicuous and omnipresent properties of the microscopic world, but the majority of states allowed by quantum physics are not seen in the macroscopic world. This has led the founders of quantum mechanics to raise important questions regarding the classical limit of this theory.

The correspondence principle was used by Niels Bohr in his paper on the model of the atom in 1913, as a tool for building the quantum theory from its expected classical limit, and explicitly formulated in 1920 [1, 2]. In a paper published in 1917 [3], Albert Einstein proposes a generalization to integrable multidimensional systems of the Bohr–Sommerfeld–Epstein quantization rule. He notes however that non-integrable systems cannot be quantized in this way, which implies that the route from a quantum model, based on the linear Schrödinger equation, to the corresponding classical chaotic system, is far from trivial.

In 1926, Erwin Schrödinger considers the quantum solution for the eigenstates of the harmonic oscillator, [4] and argues that 'at first sight it appears very strange to try to describe a process, which we previously regarded as belonging to particle mechanics, by a system of such proper vibrations'. He then demonstrates that 'a group of proper vibrations' of high quantum number n and of relatively small quantum-number differences may represent a particle executing the motion expected from usual mechanics, i.e. oscillating with a constant frequency—these are the coherent states, subsequently studied by Roy Glauber with great detail [5, 6]. Schrödinger goes back to this question in 1935. In his critical appraisal on the status of quantum mechanics [7], he argues, with his famous cat example, that the existence of quantum superpositions in the microscopic world imply that they must also exist in the macroscopic world. He realizes then a fundamental distinction between this new situation and the one considered by him in 1926: 'an uncertainty originally restricted to the atomic domain has become transformed into a macroscopic uncertainty, which can be resolved through direct observation... This inhibits us from accepting in a naive way a 'blurred model' as an image of reality.... There is a

difference between a shaky or not sharply focused photograph and a photograph of clouds and fogbanks'.

Albert Einstein, in a letter to Max Born in 1954 [8], considers a fundamental problem of quantum mechanics the inexistence at the classical level of the majority of states allowed by quantum mechanics, namely coherent superpositions of two or more macroscopically localized states. He argues, in that letter: 'let ψ_1 and ψ_2 be two solutions of the same Schrödinger equation. Then $\psi = \psi_1 + \psi_2$ also represents a solution of the Schrödinger equation, with equal claim to describe a possible real state. When the system is a macro system, and when ψ_1 and ψ_2 are 'narrow' with respect to the macro-coordinates, then in by far the greater number of cases, this is no longer true for ψ. Narrowness in regard to macro-coordinates is a requirement which is not only independent of the principles of quantum mechanics, but, moreover, incompatible with them'.

Decoherence induced by the interaction with the environment plays an important role in the understanding of these fundamental questions [9–11]. This interaction leads to loss of coherence and entanglement. The dynamics of this decoherence process is thus related to the elusive boundary between the quantum and the classical world. It also has strong implications for a practical question: the robustness of quantum computers, which depend on the resilience of coherence and entanglement.

The recent development of methods to study the quantum mechanical behavior of individual atoms and photons has allowed the experimental investigation of the dynamics of decoherence [12, 13] and, in particular, of the dynamics of entanglement in open systems [14–28]. Furthermore, in the last few years, experiments with light have led to the realization of multi-partite entangled states, up to 10 000 entangled modes [29], or up to 3000 atoms entangled with the intermediation of a single photon [30]. This opens new frontiers both for applications in quantum information and for new explorations into the frontiers of quantum mechanics. In particular, as will be shown in this paper, optical setups allow the investigation of subtle decoherence phenomena, which help to throw some light on the quantum–classical transition.

This article reviews some of these developments, with emphasis on the investigations with which I was personally involved. For a less personal, and therefore much more embracing review, focusing on the dynamics of entanglement in open systems, see [28].

2. Schrödinger cats and the decay of coherence

The first experimental probe of the environment-induced quantum–classical transition was realized in 1996 [12]. The basic tools were a microwave cavity formed by superconducting mirrors (with damping times τ that reach, nowadays, a fraction of a second, corresponding to a quality factor $Q = \omega\tau$ of the order of 10^{10}), and a beam of Rydberg atoms. The experimental setup is sketched in figure 1.

The superconducting cavity is fed by a microwave generator, which injects a coherent state into the cavity.

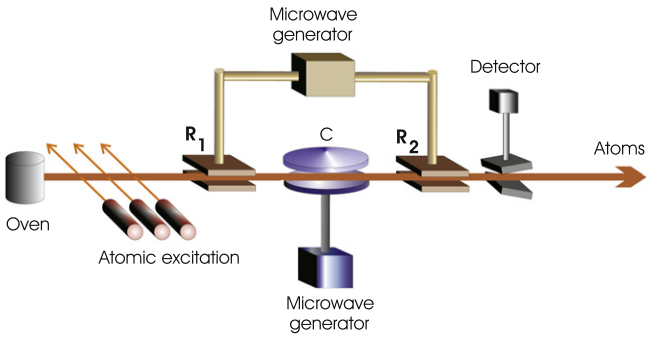

Figure 1. Experimental arrangement for producing and measuring a coherent superposition of two coherent states of the field in cavity **C**.

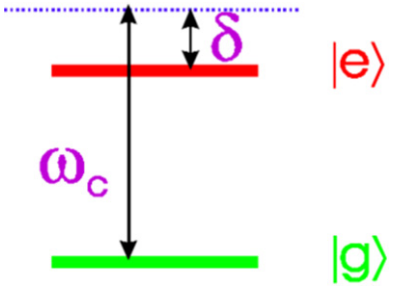

Figure 2. Atomic level scheme for the production and measurement of a coherent superposition of two coherent states of the electromagnetic field in a cavity: the transition $g \leftrightarrow e$ is detuned by δ from the frequency ω_C of a mode of cavity C, and is resonant with the fields in $\mathbf{R}_1$ and $\mathbf{R}_2$.

Rubidium atoms are excited by a combination of laser and microwave fields to a high-lying level, with a valence electron in a circular orbit seeing a shielded core, a system that can be considered, within a good approximation, a hydrogenoid atom. The corresponding principal quantum number is of the order of 50 and the orbital angular momentum quantum number is $\ell = 49$, which implies that this excited state has a long lifetime (of the order of 30 ms). The transition dipoles for these excited states are huge, of the order of 1000 atomic units.

The experiment involves three main steps: (i) the electromagnetic field in the superconducting cavity is prepared in a single-mode (frequency ω) coherent state, as mentioned above; (ii) the Rydberg atoms, previously excited to a state $|e\rangle$, cross successively a low-Q cavity ($\mathbf{R}_1$ in figure 1), the superconducting cavity **C** and another low-Q cavity $\mathbf{R}_2$; (iii) the atomic state is detected. The low Q of $\mathbf{R}_1$ and $\mathbf{R}_2$ implies that the field inside these cavities can be considered as classical, even though it has an average photon number of the order of one [31]. This field prepares a coherent superposition of two Rydberg states $|e\rangle$ and $|g\rangle$.

The relevant atomic levels are sketched in figure 2. The transition $g \leftrightarrow e$, corresponding to frequency ω_{ge}, is detuned by $\delta = \omega_C - \omega_{ge}$ from the cavity mode with frequency ω_C, so that the atom has a dispersive interaction with the field. Under this condition, the action of the atom on the field can be considered as that of a single-atom refraction index, which induces a phase change in the field. The frequency shift ϕ can

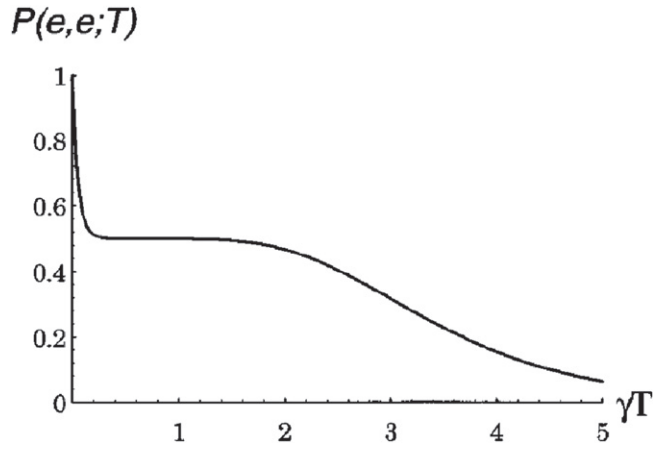

Figure 3. Probability of detecting the second atom in state $|e\rangle$ if the first atom is detected in this state. There is a fast decay to the value 0.5, corresponding to the transformation of the coherent superposition of two coherent states of the field into a statistical mixture, followed by a slow decay, corresponding to the decay of each coherent state in the mixture.

be obtained from second-order perturbation theory: states $|e\rangle$ and $|g\rangle$ shift the phase of the coherent state $|\alpha\rangle$ in opposite directions by $\phi = \Omega_0^2 t_{\rm int}/4\delta$, i.e. the product of the Stark shift per photon and the interaction time $t_{\rm int}$ between the atom and the cavity field. Therefore, after the atom exits cavity C, the combined atom-field system is represented by the state $[|e\rangle|\alpha\exp(i\phi)\rangle + |g\rangle|\alpha\exp(-i\phi)\rangle]/\sqrt{2}$, which can be considered as a realization of the typical measurement model, as discussed by von Neumann [32]: the two coherent states with different phases mimic two different positions of the pointer in a measuring apparatus, correlated with two different states of the atom. The action of $\mathbf{R}_2$ implies that this state becomes $\{|e\rangle[|\alpha\exp(i\phi)\rangle - |\alpha\exp(-i\phi)\rangle] + |g\rangle[|\alpha\exp(i\phi)\rangle + |\alpha\exp(-i\phi)\rangle]\}/\sqrt{2}$. Detection of the atom in state $|e\rangle$ or $|g\rangle$, through an ionization detector, projects therefore the field onto a superposition of two coherent states with different phases, an example of a 'Schrödinger cat'-like state.

Decoherence is probed by a second atom, sent in the same initial state as the first one through the three-cavity setup [33, 34]. Figure 3 illustrates, for the special case $\phi = \pi/2$, the behavior of the correlation probability $P(e, e; T)$ of finding the second atom in the excited state, if the first one was detected in this state, as a function of γT, where γ is the decay rate of the field in the cavity and T is the time interval between the two detections. In the absence of noise, there is perfect correlation between the detection of the first and second atom: the second atom is found in the same state as the first one. However, noise affects the coherence, the more so the longer it takes for the probing atom to arrive [34], as shown in figure 3. The fast decay of the correlation to the value $1/2$, exhibited in this figure, signalizes the loss of coherence between the two coherent states $|\alpha\exp(i\phi)\rangle$ and $|\alpha\exp(-i\phi)\rangle$, the state becoming the mixture $[|\alpha\exp(i\phi)\rangle\langle\alpha\exp(i\phi)| + |\alpha\exp(-i\phi)\rangle\langle\alpha\exp(-i\phi)|]N$, where N is a normalization constant. This dynamics was verified experimentally [12]. The decay of coherence is exponential, within a very good approximation, with a lifetime equal to the damping time of the cavity field divided by $d^2/2$, where $d = 2|\alpha|\sin^2(\phi/2)$ is the distance between the two phasors $\alpha\exp(i\phi)$ and $\alpha\exp(-i\phi)$ in phase space. The larger the average number of photons $\langle n\rangle = |\alpha|^2$ in the initial coherent state, the larger is this distance, and the faster is the decoherence. For large average photon numbers, this time scale is much smaller than the one corresponding to the decay of the field in the cavity, which in figure 3 corresponds to the tail of the correlation function.

This behavior, which characterizes the quantum–classical transition in this case, is a conspicuous trait of the quantum world, which explains the inexistence at the classical level of the majority of states allowed by quantum mechanics, namely coherent superpositions of two or more macroscopically localized states: 'Schrödinger cats' have very short lives, the shorter the fatter they are... On the other hand, coherent states are much more robust, deserving the name 'pointer states' [10], as suggested by the analogy with a measuring device.

This analysis is relevant for understanding how classical chaotic dynamics may emerge from quantum systems, described by the linear Schrödinger equation. Decoherence plays again a major role in driving the quantum system towards classical trajectories in phase space [35–40]. For a quantum system that has a classically chaotic limit, the evolution in phase space generates quantum superpositions with characteristic interference fringes, which are damped out through the interaction with the environment, leading to classical trajectories as the typical action corresponding to the quantum state becomes much larger than the Planck constant [39].

My involvement in these research themes, plus my early contributions to the analysis of deviations from exponential decay in atomic physics [41, 42], led me to consider an analogous problem concerning entanglement: How robust should it be under the influence of the environment? Is the decay law exponential? How does this decay scales with the number of particles? These questions will be addressed in the following sections.

3. Two-qubit entanglement and non-exponential decay

3.1. Measures of entanglement

Regarding entanglement, Schrödinger made a deep statement in one of his 1935 papers [7], which offers a clue for defining a measure of entanglement: 'this is the reason that knowledge of the individual systems can decline to the scantiest, even zero, while that of the combined system remains continually maximal. Best possible knowledge of a whole does not include best possible knowledge of its parts—and that is what keeps coming back to haunt us'. Ignorance about parts of an entangled system is a hallmark of entanglement. This

suggests defining an entropic measure for the entanglement of a pure state.

Entanglement is usually defined by its opposite: a state is entangled if it is not separable. A separable pure state of n parties can be written as a product of the states of the parties:

$$|\Psi_{12\ldots n}\rangle = |\psi_1\rangle \otimes |\psi_2\rangle \otimes \ldots |\psi_n\rangle, \quad (1)$$

while a separable mixed state of n parties can be written as

$$\rho_{12\ldots n} = \sum_\mu p_\mu \rho_1^\mu \otimes \rho_2^\mu \otimes \ldots \rho_n^\mu, \quad 0 \leqslant p_\mu \leqslant 1, \quad (2)$$

meaning that, with probability p_μ, it can be found in the product state $\rho_1^\mu \otimes \rho_2^\mu \otimes \ldots \rho_n^\mu$.

For pure states, two possible measures are the Von Neumann entropy corresponding to the reduced density matrix ρ_r of one of the parts, $S_{\rm N}(\rho_r) = -{\rm Tr}[\rho_r \log_2 \rho_r]$, and the linear entropy $S_{\rm L}(\rho_r) = 2(1 - {\rm Tr}\rho_r^2)$. Both definitions lead to the value zero if the global pure state of the system is a product of the states of its parts, since then each part is a pure state. One has in this case a separable (non-entangled) state. The normalization is chosen so that, for two qubits, both entropies have a maximum value equal to one, corresponding to maximal ignorance about the state of each part. This defines the maximally entangled states of two qubits, for which $\rho_r = (1/2)\mathbb{1}$, where $\mathbb{1}$ is the unit 2×2 matrix. So are the Bell states: $|\Psi^\pm\rangle = ([|0\rangle_A \otimes |1\rangle_B \pm |0\rangle_A \otimes |1\rangle_B)/\sqrt{2}$, $|\Phi^\pm\rangle = ([|0\rangle_A \otimes |0\rangle_B \pm |1\rangle_A \otimes |1\rangle_B)/\sqrt{2}$, where $|0\rangle$ and $|1\rangle$ are orthogonal states of a two-level system.

These measures do not work however for mixed states, for which ignorance of the state of each party does not correspond necessarily to entanglement. Equation (2) implies that the state of each party is not completely known, even though the global state is separable.

If the global state of a system can be decomposed as in (2), the state is separable. However, it is usually very difficult to find such a decomposition for a general state.

A necessary condition for separability was first noted by Asher Peres [43]. It is based on the operation of partial transposition, which is not positive-definite, as opposed to the transposition of a matrix. According to Peres, if ρ is separable, then the partially transposed matrix is positive, that is, the density operator has a positive partial transpose (PPT):

$$\rho_{12\ldots n}^{T_i} = \sum_\mu p_\mu \rho_1^\mu \otimes \ldots \otimes (\rho_i^\mu)^{\rm T} \otimes \ldots \rho_n^\mu, \quad (3)$$

which follows immediately from the fact that the transposition of the density matrix ρ_i^μ does not change its eigenvalues.

This condition was shown to be necessary and sufficient for bipartite 2×2 and 2×3 systems by the Horodecki family [44]. For higher dimensions, it is possible to find PPT states that are entangled.

These criteria have led to the definition of a measure of entanglement, called *negativity* [45, 46]. It is defined by the expression

$$\mathcal{N}(\rho_{AB}) \equiv 2\sum_i |\lambda_{i-}|, \quad (4)$$

where λ_{i-} are the negative eigenvalues of the partially transposed matrix. The normalization is chosen so that $\mathcal{N} = 1$ for a Bell state. It is clear from the above comments that, for dimensions higher than 6, $\mathcal{N} = 0$ does not imply separability. Entangled states for which $\mathcal{N} = 0$ are said to have *bound entanglement* [47], designation corresponding to the fact that they cannot be transformed into maximally entangled states through distillation operations.

For two qubits, Wootters [48] introduced another measure of entanglement, the concurrence $\mathcal{C}$, given by

$$\mathcal{C} = \max\{0, \Lambda\}, \quad (5)$$

where

$$\Lambda = \sqrt{\lambda_1} - \sqrt{\lambda_2} - \sqrt{\lambda_3} - \sqrt{\lambda_4}, \quad (6)$$

and the λ_i's are the eigenvalues, in decreasing order of magnitude, of the matrix $\rho(\sigma_y^A \otimes \sigma_y^B)\rho^*(\sigma_y^A \otimes \sigma_y^B)$, the conjugation operation being done in the computational basis $\{|00\rangle, |01\rangle, |10\rangle, |11\rangle\}$, where $|00\rangle \equiv |0\rangle_A \otimes |0\rangle_B$. For separable states, $\mathcal{C} = 0$, while $\mathcal{C} = 1$ for maximally entangled states. For pure states, $\mathcal{C}$ reduces to the square root of the linear entropy: $\mathcal{C} = \sqrt{2(1 - {\rm Tr}\rho_r^2)}$.

These measures should not be taken, however, as a tool for comparing entanglement of different states. Indeed, the ordering of entangled states depends on the measure. As shown in [49], states with the same negativity may have different concurrences, and vice versa. However, all measures are defined so that they vanish for separable states.

3.2. Probing the dynamics of entanglement with light

The decay of entanglement may be remarkably different from that of coherence. As shown by several authors [50–56], entanglement may vanish at finite times, with non-exponential decay, before coherence disappears.

Here we discuss this peculiar dynamics within the framework of a paradigmatic example: the spontaneous decay of a two-level atom [55]. Each qubit of an entangled pair corresponds to a two-level atom, with excited and ground states $|e\rangle$ and $|g\rangle$, respectively. The dynamics of each atom is described by the the system of equations

$$\begin{aligned} &|g\rangle_{\rm S} \otimes |0\rangle_{\rm E} \rightarrow |g\rangle_{\rm S} \otimes |0\rangle_{\rm E} \\ &|e\rangle_{\rm S} \otimes |0\rangle_{\rm E} \rightarrow \sqrt{1-p}\,|e\rangle_{\rm S} \otimes |0\rangle_{\rm E} + \sqrt{p}\,|g\rangle_{\rm S} \otimes |1\rangle_{\rm E}, \end{aligned} \quad (7)$$

where, for a decaying atom, $p = 1 - \exp(-\Gamma t)$. The subscript S stands for system, while E stands for environment. With this choice of p, the above system of equations—usually named 'amplitude channel' or 'amplitude map'—is essentially the one derived by Weisskopf and Wigner in 1930 [57]. The first equation above states that, if the atom is in the ground state, and there are no photons in the environment, then the global state does not change. The second equation corresponds to the situation in which the atom is initially in the excited state, and the field (environment) is in the vacuum state. There is then a probability p that the atom decays, releasing one photon into the environment, and a probability $1 - p$ that it remains in the initial state. The solution of the above equation, traced out with respect to the environment, coincides with the result obtained from the usual master

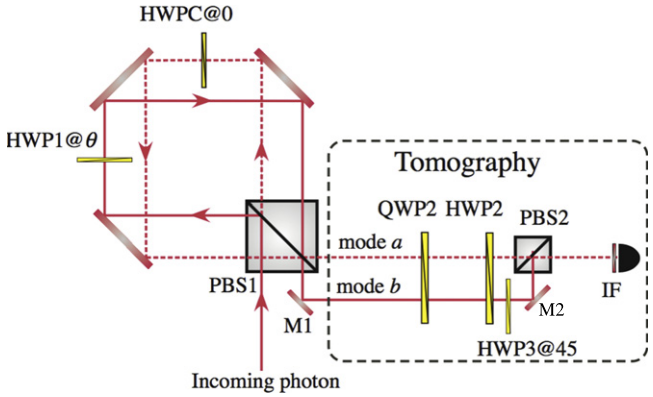

Figure 4. Realization of amplitude map with photons. The polarized beam splitter PBS1 reflects vertically polarized light (full-line path coming out of PBS1), and lets the horizontal component go through (dashed-line path coming out from PBS1). The half-wave plate HWP1 turns the vertical polarization by the angle 2θ, while HWPC compensates for the path difference introduced by HWP1, without changing the horizontal polarization of the photon that takes this path. QWP2 is a quarter-wave plate, which together with the half-wave plates HWP2 and HWP3 is used for the tomographic reconstruction of the polarization state. Spatial modes a and b are recombined incoherently in PBS2, by introducing a path difference larger than the coherence length, with the help of mirrors M1 and M2. Adapted from [14].

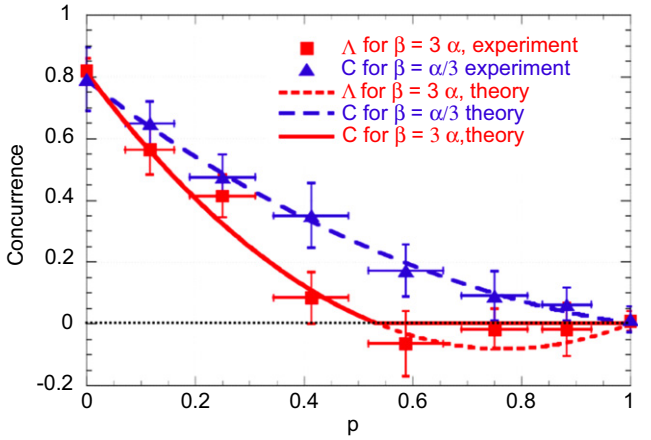

Figure 5. Experimental demonstration of the dynamics of entanglement. When the population of the excited state is larger than that of the ground state, entanglement vanishes for values of the decay probability smaller than one, corresponding to finite times. Adapted from [14].

equation for the decay of a two-level atom, in the Markovian approximation.

One should note, however, that the same set of equations could be used to describe an atom interacting with a single mode of the electromagnetic field in a cavity, by setting $p = \cos^2(\Omega t/2)$, where Ω is the Rabi frequency. It is more general, therefore, to consider the evolution of the system as a function of p, rather then t. This is the strategy adopted in [14].

Starting with a generic two-qubit entangled state, one applies the above evolution to each of the two qubits, one traces out the environment, thus finding the evolution of the two-qubit reduced density matrix, from which one calculates either the negativity or the concurrence. If one takes for definiteness the initial two-qubit state as

$$|\Psi(0)\rangle = \alpha|gg\rangle + \beta|ee\rangle, \tag{8}$$

then the concurrence, which in this case coincides with the negativity for all values of p, is given by

$$\mathcal{C} = \max\{0,\, 2(1-p)|\beta|(|\alpha| - p|\beta|)\}. \tag{9}$$

The initial concurrence, corresponding to $p = 0$, is $\mathcal{C} = 2|\alpha\beta|$. States with the same initial concurrence may display however very different behavior. If the initial population of the excited state is not larger than that of the ground state, that is, if $|\beta| \leqslant |\alpha|$, then the concurrence vanishes only for $p = 1$, which corresponds to infinite times if $p = 1 - \exp(-\Gamma t)$. If instead $|\beta| > |\alpha|$, then the concurrence vanishes for $p = |\alpha/\beta|$, that is, entanglement vanishes for finite times, even though coherence still survives. This characteristic trait of the dynamics of entanglement was named 'sudden-death' [58].

This peculiar behavior of the dynamics of entanglement was demonstrated experimentally in [14], by using twin-photon beams generated by shining UV laser light on a nonlinear crystal. The experimental scheme used to realize an amplitude map is displayed in figure 4. The main idea is to associate the states of a two-level atom with the horizontal and vertical polarization of a photon, and the two states of the environment in equation (7) with distinct spatial paths. The coupling between polarization and path is provided by polarized beam splitters (PBS): a horizontally polarized photon goes through the PBS, which reflects a vertically polarized photon.

Figure 4 displays a Sagnac-like interferometer and the path followed by an initially horizontally polarized photon (dashed line), which comes out in the spatial mode a, corresponding to state $|0\rangle_{\rm E}$ of the environment. This trajectory mimics the first equation in (7). On the other hand, a vertically polarized photon is reflected by PBS1, and if the half-wave plate HWP1 is absent, follows the full-line path, emerging also in the spatial mode a. This is a realization of the second equation in (7), for the special case $p = 0$. Generalization for $p \neq 0$ amounts to inserting the optical element HWP1 (together with HWPC, which compensates for the path difference introduced by HWP1). HPW1 transforms the state of a vertically polarized photon into the superposition $\cos 2\theta|V\rangle + \sin 2\theta|H\rangle$. The H component of this state emerges in mode b, corresponding to state $|1\rangle_{\rm E}$ of the environment. Therefore, the polarization of an initial vertically polarized photon becomes entangled with the path, $|V\rangle|0\rangle_{\rm E} \rightarrow \sqrt{1-p}\,|V\rangle|0\rangle_{\rm E} + \sqrt{p}\,|H\rangle|1\rangle_{\rm E}$, with $p = \sin^2(2\theta)$, thus realizing the second line of (7). Polarization tomography is realized by joining the two paths incoherently, which amounts to tracing out the environment (path) degrees of freedom.

This setup is duplicated, so that each photon of an initial entangled state is submitted to its own amplitude map. Coincidence joint polarization tomography is realized on the

photon pairs, and the concurrence is calculated from the reconstructed density matrix, by using equations (5) and (6). The experimental results are displayed in figure 5, together with the theoretical curves obtained by applying the theoretical map to the initial experimental entangled state, which is very well approximated by the expression (8), with α and β real. Different relations between the coefficients α and β in (8) are considered. Note that, even though Λ, defined by (6), and obtained from the tomographically reconstructed polarization state, may be negative, the concurrence C, defined by (5), is always positive, and it vanishes for values of p smaller than one if the initial state is such that $|\alpha| < |\beta|$.

4. Entanglement dynamics for multipartite states

An important question, both for practical applications of entanglement, and for probing the boundary between quantum and classical physics, is the scaling behavior of the decay of entanglement with the number of qubits.

A detailed study of the dynamics of the class of states $|\Psi\rangle = \alpha|0\rangle^{\otimes N} + \beta|1\rangle^{\otimes N}$, where $|0\rangle^{\otimes N}$ stands for the tensor product of N states $|0\rangle$, was developed in [59]. These states generalize the Greenberger–Horne–Zeilinger (GHZ) state $(|000\rangle + |111\rangle)/\sqrt{2}$, defined in [60]. In [59], each qubit interacts with its own independent environment. Several kinds of environment were considered: amplitude decay, corresponding to the map (7), depolarization, dephasing, and thermal environments.

Peculiar features of the dynamics emerged from that study. For instance, it was shown that, for these generalized GHZ states, the vanishing of the negativity, for a given partition of the state, implies the separability of this partition. Furthermore, it was shown that the finite-time disappearance of entanglement is verified also for this generalized situation, but with a surprising caveat: the 'sudden-death' time approaches infinity as the number of qubits increases! Thus, for amplitude damping, with $|\alpha/\beta| < 1$, the negativity vanishes for all bipartitions k: $N - k$ when the transition probability reaches the critical value $p_c = |\alpha/\beta|^{2/N}$, which is independent of k. Furthermore, as shown in [59], the state becomes fully separable at this point. One notes however that $p_c \to 1$ when $N \to \infty$, so the disentanglement time goes to infinity as the number of qubits increases! Does this result imply that entanglement becomes more robust as N increases? This would be a strange conclusion, since one would expect that as N increases quantum features should get more fragile.

This apparent paradox is resolved by examining the full evolution of the state [59]. Figure 6 displays, for the depolarizing channel, the negativities as functions of p corresponding to the balanced partitions $N/2 : N/2$, for several values of N, with the inset showing the behavior of the negativities in the region where the entanglement vanishes for the $N = 4$ state. The inset displays the behavior noted above for the amplitude channel: as N increases, the disentanglement time also increases. However, the full plot shows that, as the number of qubits increases, the decay of entanglement becomes faster, implying that the negativity becomes

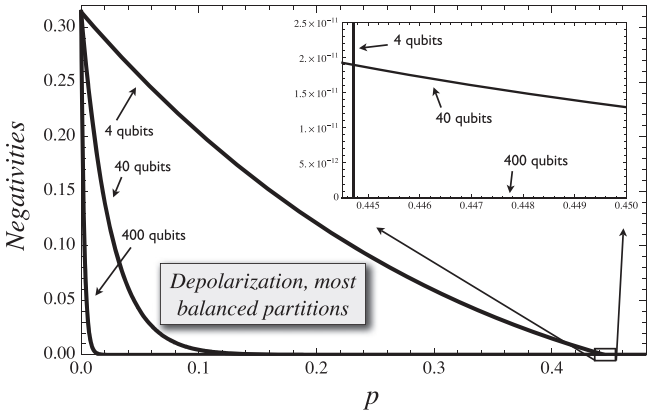

Figure 6. Negativities versus p for $N = 4$, 40 and 400, for the depolarization channel and for the most balanced partitions. The initial state is taken as $|\Psi\rangle(0) = (1/3)|0\rangle^{\otimes N} + (8/3)|1\rangle^{\otimes N}$. The inset shows a magnification of the region in which the negativity for the state with 4 qubits vanishes. Even though the negativities for the states with 40 and 400 qubits cross the latter and vanish much later, they become orders of magnitude smaller than their initial value long before reaching the crossing point. Reproduced with permission from [59]. Copyright American Physical Society 2008.

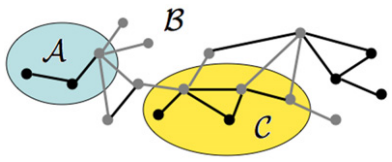

Figure 7. Example of a mathematical graph. The corresponding physical state is obtained by associating each vertex with a qubit in the state $|+\rangle = (|0\rangle + |1\rangle)/\sqrt{2}$, and applying controlled-Z gates on adjacent qubits. A possible partition of this graph is diplayed, splitting the system in three parts $\mathcal{A}$, $\mathcal{B}$, and $\mathcal{C}$. The vertices and edges in gray correspond respectively to the *boundary qubits* and the *boundary-crossing edges*. Reproduced with permission from [61]. Copyright American Physical Society 2009.

negligible much before it vanishes. In this region, the tiny amount of entanglement still remaining is extremely susceptible to extra noise, which can be taken as a manifestation of the classical limit in this case.

The generalization of this study for graph states was carried out in [61, 62]. Graph states are defined in the following way. Consider a mathematical graph consisting of vertices and edges connecting the vertices. Associate to each vertex a qubit, in the state $|+\rangle = (|0\rangle + |1\rangle)/\sqrt{2}$. Apply, between two states in adjacent vertices i and j (that is, connected by an edge) a 'controlled Z' operation: $(|0\rangle + |1\rangle)_i \otimes (|0\rangle + |1\rangle)_j \to |0\rangle_i|0\rangle_j + |0\rangle_i|1\rangle_j + |1\rangle_i|0\rangle_j - |1\rangle_i|1\rangle_j$. The resulting state is a graph state. It has been shown to be a basic resource in measurement-induced quantum computation [63]. An example is given in figure 7.

Light has been a useful resource to build graph states. In particular, quantum optical frequency combs have been used to build multipartite graph states involving tens of modes [64, 65].

In [61, 62] it was shown that graph-state entanglement is particularly resilient to the deleterious effects of the environment. For a large class of quantum channels and entanglement quantifiers, lower bounds for entanglement were shown to depend only on boundary qubits (connected by gray lines in figure 7). Inner qubits, represented by black dots in figure 7 do not contribute to the lower bounds, thus mitigating the scaling of the decay with the number of qubits.

Further resistance to decoherence can be reached by exploring, through quantum control, non-Markovian features of the interaction between multi-partite systems and the environment [66, 67]. Global coupling to a common environment, as opposed to the individual environments considered here, may also lead to environment-induced entanglement [68] or even the generation of macroscopic superpositions of quantum states [69].

5. Decoherence and the flow of entanglement: probing the environment with optical setups

A subtle question regarding the dynamics of entanglement concerns the imprint of an initially entangled state into the environment. It was argued by Zurek [70] that the detailed study of the environment uncovers essential traits of the classical world. In particular, classical-like states, the so-called pointer states mentioned in section 2, lead to the proliferation, in the environment, of multiple records of these states, as opposed to superpositions of pointer states. It it this multitude of copies that allows us to obtain relevant information on those states without having to re-prepare them, by using the information already present in the environment. This has been named by Zurek 'quantum Darwinism,' term associated with the resilience of pointer states: only quantum states that leave multiple records in the environment can be observed on the macroscopic scale.

The perspective is quite different however when one deals with entanglement, an intrinsic quantum phenomenon. Then, the question is: What is the effect of an initial entangled state on its environment? As the original entanglement decays, what kinds of entanglement show up in the environment, and between the system and the environment?

These questions have been investigated recently in a series of experimental papers [24–27]. They were based on the realization, already discussed in [16], that a simple modification of the setup displayed in figure 4 allows the joint tomography of polarization and path, as shown in figure 8. Since only two states of the environment show up in (7), the states $|0\rangle_E$ and $|1\rangle_E$, it can be considered as a qubit, and therefore the joint tomography is equivalent to the reconstruction of the state of four qubits, two of which are initially entangled.

When twin photons are sent through the respective Sagnac interferometers, the initial entanglement gets transferred to the corresponding paths [27]. The polarization-path tomography [27] demonstrates that the disappearance of polarization entanglement is mediated by the appearance of genuine multipartite entanglement, that is, a joint system-environment state that is not biseparable. Recognition of genuine multipartite entanglement is made by adapting a fidelity witness defined in [71]: whenever the fidelity $\mathcal{F} = \langle \mathcal{D}|\rho|\mathcal{D}\rangle$ of the measured state ρ with respect to the state

$$|\mathcal{D}\rangle = (1/\sqrt{6})(|0000\rangle + |1111\rangle + |0011\rangle + |0110\rangle + |1001\rangle) \quad (10)$$

is larger than $2/3$, the state has genuine four-partite entanglement. The fidelities for the experimentally reconstructed ρ are shown in figure 9. In the interval

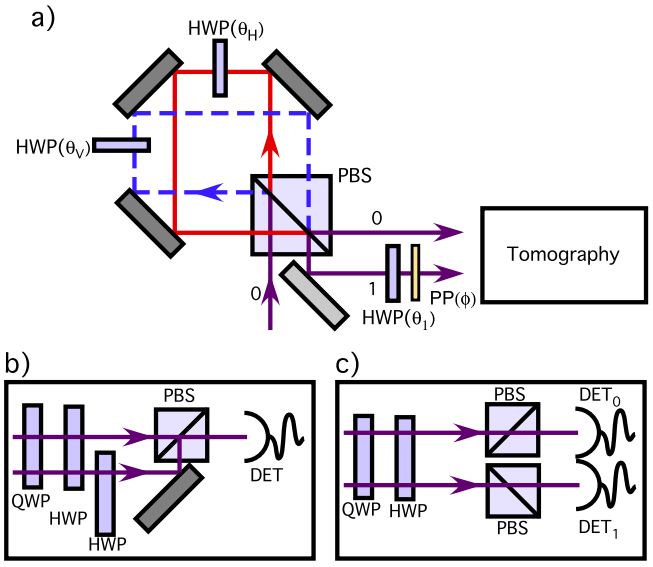

Figure 8. Variation of the setup shown in figure 4, allowing the joint tomography of polarization and path. The two outgoing paths from the interferometer shown in (a), previously combined incoherently, as shown in (b), are now separated, as shown in (c), and can thus be measured independently. Reproduced with permission from [16]. Copyright American Physical Society 2008.

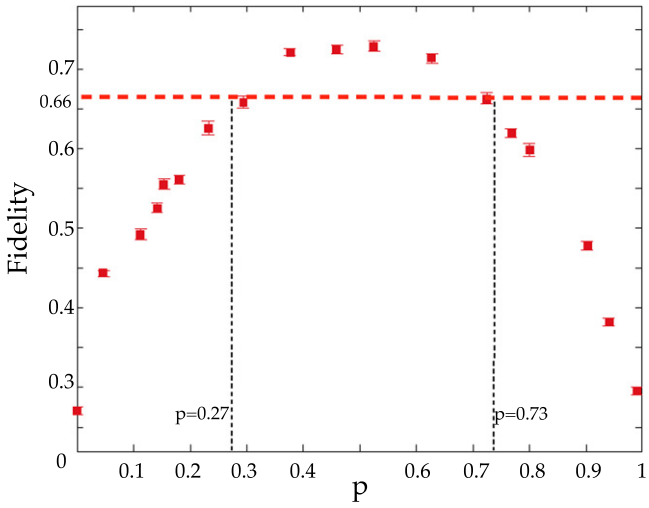

Figure 9. Fidelity between the experimentally reconstructed system-environment density matrix and the state $|\mathcal{D}\rangle$ defined in (10), as function of p. Genuine four-partite entanglement is detected in the region $p \in (0.27, 0.73)$. Adapted from [27].

$p \in (0.27, 0.73)$, the fidelities exceed $2/3$, demonstrating the presence of genuine four-partite entanglement.

6. Conclusion

In this paper, we have reviewed some work that is related to the use of electromagnetic radiation in the microwave and optical spectra in order to explore subtle questions related to the emergence of the classical world from quantum physics. Decoherence plays a major role in all the work reviewed here: the environment rules the transition from quantum to classical. Technically demanding experiments have helped to explore some aspects of this question, including the scaling of decoherence and disentangling with the 'size' of the system, which is related to the number of its constituents (number of photons, number of qubits).

The relationship between the quantum and the classical world is a long-standing theme in physics, since the inception of quantum mechanics. The theory of decoherence explains important aspects of this subject, but many open questions remain.

Recent contributions have unveiled relations between quantum and classical descriptions of nature, revisiting the derivation of the Schrödinger equation [72] and obtaining a wave equation that interpolates between classical and quantum mechanics [73].

Full understanding of the emergence of the classical world from the quantum substrate is still far from being attained. Light may again come to the rescue: optomechanical experiments [74, 75] may help to elucidate the role of gravitation in decoherence, a topic which up to now is very little understood. It is related to one of the most challenging problems of this century: the connection between quantum theory and general relativity.

Acknowledgments

The author would like to thank the several collaborators that greatly influenced his views on the dynamics of coherence and entanglement. In particular, he would specially like to thank A Acín, G H Aguilar, M P Almeida, L Aolita, A Auyuanet, M Brune, A Büchleitner, A R R Carvalho, D Cavalcanti, R Chaves, J H Eberly, M França Santos, S Haroche, M Hor-Meyll, O Jiménez Farías, R L de Matos Filho, F de Melo, P Milman, F Mintert, H M Nussenzveig, J-M Raimond, A Salles, P H Souto Ribeiro, F Toscano, A Valdés-Hernández, S P Walborn, and N Zagury.

This work was partially funded by the Brazilian National Institute for Science and Technology on Quantum Information, and the Brazilian funding agencies CNPq, FAPERJ, and CAPES.

References

[1] Bohr N 1920 *Z. Phys.* **2** 423
[2] Nielsen J R (ed) 1976 *The Correspondence Principle (1918-1923)* (*Niels Bohr Collected Works* vol 3) (Amsterdam: North-Holland)
[3] Einstein A 1917 *Verh. Dtsch. Phys. Ges.* **19** 82
[4] Schrödinger E 1926 *Naturwissenschaften* **28** 664
[5] Glauber R J 1963a *Phys. Rev.* **130** 2529
[6] Glauber R J 1963b *Phys. Rev.* **131** 2766
[7] Schrödinger E 1935 *Naturwissenschaften* **23** 807
[8] Born M 2005 *The Born–Einstein Letters: Friendship, Politics and Physics in Uncertain Times* (London: Macmillan)
[9] Zurek W H 1991 *Phys. Today* **44** 36
[10] Zurek W H 2003 *Rev. Mod. Phys.* **75** 715
[11] Joos E, Zeh H D, Kiefer C, Giulini D, Kupsch J and Stamatescu I O 2003 *Decoherence and the Appearance of a Classical World in Quantum Theory* (Berlin: Springer)
[12] Brune M, Hagley E, Dreyer J, Maître X, Maali A, Wunderlich C, Raimond J M and Haroche S 1996 *Phys. Rev. Lett.* **77** 4887
[13] Myatt C J, King B E, Turchette Q A, Sackett C A, Kielpinski D, Itano W M, Monroe C and Wineland D J 2000 *Nature* **403** 269
[14] Almeida M P, Melo F d, Hor-Meyll M, Salles A, Walborn S P, Ribeiro P H S and Davidovich L 2007 *Science* **316** 579
[15] Laurat J, Choi K S, Deng H, Chou C W and Kimble H J 2007 *Phys. Rev. Lett.* **99** 180504
[16] Salles A, Melo F d, Almeida M P, Hor-Meyll M, Walborn S P, Ribeiro P H S and Davidovich L 2008 *Phys. Rev.* A **78** 022322
[17] Farías O J, Latune C L, Walborn S P, Davidovich L and Ribeiro P H S 2009 *Science* **324** 1414
[18] Papp S B, Choi K S, Deng H, Lougovski P, van Enk S J and Kimble H J 2009 *Science* **324** 764
[19] Barreiro J T, Schindler P, Gühne O, Monz T, Chwalla M, Roos C F, Hennrich M and Blatt R 2010 *Nat. Phys.* **6** 943
[20] Coelho A S, Barvosa F A S, Cassemiro K N, Villar A S, Martinelli M and Nussenzveig P 2009 *Science* **326** 823
[21] Xu J-S, Li C-F, Gong M, Zou X-B, Shi C-H, Chen G and Guo G-C 2010 *Phys. Rev. Lett.* **104** 100502
[22] Barbosa F A S, Coelho A S, de Faria A J, Cassemiro K N, Villar A S, Nussenzveig P and Martinelli M 2010 *Nat. Photon.* **4** 858
[23] Monz T, Schindler P, Barreiro J T, Chwalla M, Nigg D, Coish W A, Harlander M, Hänsel W, Hennrich M and Blatt R 2011 *Phys. Rev. Lett.* **106** 130506
[24] Farías O J, Valdés-Hernández A, Aguilar G H, Ribeiro P H S, Walborn S P, Davidovich L, Qian X-F and Eberly J H 2012 *Phys. Rev.* A **85** 012314
[25] Farías O J, Aguilar G H, Valdés-Hernández A, Ribeiro P H S, Davidovich L and Walborn S P 2012 *Phys. Rev. Lett.* **109** 150403
[26] Aguilar G H, Farías O J, Valdés-Hernández A, Ribeiro P H S, Davidovich L and Walborn S P 2014 *Phys. Rev.* A **89** 022339
[27] Aguilar G H, Valdés-Hernández A, Davidovich L, Walborn S P and Ribeiro P H S 2014 *Phys. Rev. Lett.* **113** 240501
[28] Aolita L, de Melo F and Davidovich L 2015 *Rep. Prog. Phys.* **78** 042001
[29] Yokoyama S, Ukai R, Armstrong S C, Sornphiphatphong C, Kaji T, Suzuki S, ichi Yoshikawa J, Yonezawa H, Menicucci N C and Furusawa A 2013 *Nat. Photon.* **7** 982
[30] McConnell R, Zhang H, Hu J, Ćuk S and Vuletić V 2015 *Nature* **519** 439

[31] Kim J I, Romero K F, Horiguti A M, Davidovich L, Nemes M and de Toledo Piza A F R 1999 *Phys. Rev. Lett.* **82** 4737
[32] Neumann J V 1932 *Matematische Grundlagen der Quantenmechanic* (Berlin: Springer)
[33] Davidovich L, Maali A, Brune M, Raimond J M and Haroche S 1993 *Phys. Rev. Lett.* **71** 2360
[34] Davidovich L, Brune M, Raimond J M and Haroche S 1996 *Phys. Rev.* A **53** 1295
[35] Zurek W H and Paz J P 1995 *Phys. Rev. Lett.* **75** 351
[36] Berry M 2002 *Quantum Mechanics: Scientific Perspectives on Divine Action* vol 5 ed R J Russel *et al* (Berkeley, CA: Vatican Observatory and Center for Theology) p 4154
[37] Habib S, Shizume K and Zurek W H 1998 *Phys. Rev. Lett.* **80** 4361
[38] Pattanayak A K, Sundaram B and Greenbaum B D 2003 *Phys. Rev. Lett.* **90** 014103
[39] Carvalho A R R, de Matos Filho R L and Davidovich L 2004 *Phys. Rev.* E **70** 026211
[40] Toscano F, de Matos Filho R L and Davidovich L 2005 *Phys. Rev.* A **71** 010101
[41] Davidovich L 1975 *PhD Thesis* University of Rochester, Rochester, NY
[42] Davidovich L and Nussenzveig H M 1979 *Group Theoretical Methods in Physics* (*Lecture Notes in Physics* vol 94) ed W Beiglbock (Berlin: Springer) p 250
[43] Peres A 1996 *Phys. Rev. Lett.* **77** 1413
[44] Horodecki M, Horodecki P and Horodecki R 1996 *Phys. Lett.* A **223** 1
[45] Życzkowski K, Horodecki P, Sampera A and Lewenstein M 1998 *Phys. Rev.* A **58** 883
[46] Vidal G and Werner R F 2002 *Phys. Rev.* A **65** 032314
[47] Horodecki M, Horodecki P and Horodecki R 1998 *Phys. Rev. Lett.* **80** 5239
[48] Wootters W K 1998 *Phys. Rev. Lett.* **80** 2245
[49] Verstraete F, Audenaert K, Dehanene J and Moor B D 2001 *J. Phys. A: Math. Gen.* **34** 10327
[50] Rajagopal A K and Rendell R W 2001 *Phys. Rev.* A **63** 022116
[51] Życzkowski K, Horodecki P, Horodecki M and Horodecki R 2001 *Phys. Rev.* A **65** 012101
[52] Simon C and Kempe J 2002 *Phys. Rev.* A **65** 052327
[53] Diósi L 2003 *Irreversible Quantum Dynamics* (*Lecture Notes in Physics*) ed F Benatti and R Floreanini (Berlin: Springer)
[54] Dodd P J and Halliwell P J 2004 *Phys. Rev.* A **69** 052105
[55] Yu T and Eberly J H 2004 *Phys. Rev. Lett.* **93** 140404
[56] Dür W and Briegel H-J 2004 *Phys. Rev. Lett.* **92** 180403
[57] Weisskopf V and Wigner E 1930 *Z. Phys.* **63** 54
[58] Yönạ M, Yu T and Eberly J H 2006 *J. Phys. B: Atom. Mol. Opt. Phys.* **39** S621–5
[59] Aolita L, Chaves R, Cavalcanti D, Acín A and Davidovich L 2008 *Phys. Rev. Lett.* **100** 080501
[60] Greenberger D M, Horne M and Zeilinger A 1989 *Bell's Theorem Quantum Theory and Conceptions of the Universe* ed M Kafatos (Dordrecht: Kluwer) pp 69–72
[61] Cavalcanti D, Chaves R, Aolita L, Davidovich L and Acín A 2009 *Phys. Rev. Let.* **103** 030502
[62] Aolita L, Cavalcanti D, Chaves R, Dhara C, Davidovich L and Acín A 2010 *Phys. Rev.* A **82** 032317
[63] Raussendorf R and Briegel H J 2001 *Phys. Rev. Lett.* **86** 5188
[64] Chen M, Menicucci N C and Pfister O 2014 *Phys. Rev. Lett.* **112** 120505
[65] Medeiros de Araújo R, Roslund J, Cai Y, Ferrini G, Fabre C and Treps N 2014 *Phys. Rev.* A **89** 053828
[66] Gordon G and Kurizki G 2006 *Phys. Rev. Lett.* **97** 110503
[67] Álvarez G A, Rao D D B, Frydman L and Kurizki G 2010 *Phys. Rev. Lett.* **105** 160401
[68] Hor-Meyll M, Auyuanet A, Borges C V S, Aragão A, Huguenin J A O, Khoury A Z and Davidovich L 2009 *Phys. Rev.* A **80** 042327
[69] Bhaktavatsala Rao D D, Bar-Gill N and Kurizki G 2011 *Phys. Rev. Lett.* **106** 010404
[70] Zurek W H 2009 *Nat. Phys.* **5** 181
[71] Wieczorek W, Schmid C, Kiesel N, Pohlner R, Gühne O and Weinfurter H 2008 *Phys. Rev. Lett.* **101** 010503
[72] Schleich W P, Greenberger D M, Kobe D H and Scully M O 2013 *Proc. Natl Acad. Sci.* **110** 5374
[73] Schleich W P, Greenberger D M, Kobe D H and Scully M O 2015 *Phys. Scr.* **90** 108009
[74] Marshall W, Simon C, Penrose R and Bouwmeester D 2003 *Phys. Rev. Lett.* **91** 130401
[75] Aspelmeyer M, Kippenberg T J and Marquardt F 2014 *Rev. Mod. Phys.* **86** 1391